

# An Application of Particle Swarm Algorithms to Optimize Hidden Markov Models for Driver Fatigue Identification\*

Mingheng Zhang, Xiaojuan Zhai, Guang Zhao, Tonghong Chong, and Zheng Wang

**Abstract**—A hidden Markov model (HMM) has been applied to describe the dynamic process of driver fatigue over time. However, during the HMM training, the initial value selection of the confusion matrix has a great influence on the accuracy of the HMM, which brings a lot of inconveniences to the practical application. Therefore, this study applied a particle swarm optimization (PSO) algorithm to simplify the training process without affecting the accuracy of the HMM. In the beginning, an improved HMM was built based on the PSO algorithm, and then was trained by the adoption of the collected data of percentage of eye closing time over a certain period (PERCLOS), which was measured from twenty participants in a driving simulator experiment. Finally, the improved model was compared with the original model, and it didn't require the initial value selection process based on the prior condition to achieve the global optimum and improve accuracy. It indicates that the proposed method can provide an effective way for driver fatigue identification.

**Index Terms** — Driver fatigue, hidden Markov model, forward-backward algorithm, particle swarm optimization.

## I. INTRODUCTION

Driver fatigue is one of the main causes of highway accidents, especially in the large-scale traffic accidents [1]. According to the published investigation, accidents caused by driver fatigue account for 16% of all vehicle collisions, and over 20% of highway accidents are related to driver fatigue [2]. Therefore, how to accurately and effectively detect the fatigue state of drivers is a hot issue in the research field of advanced driver assistance systems (ADAS). Aiming at this problem, this paper tried to develop a driver fatigue detection method by application of an improved hidden Markov model (HMM).

In general, the existing detection methods can be roughly divided into four categories: subjective evaluations, physiological parameters [3-5], running states of vehicles [6] and driver behaviors [7]. The driver behaviors method generally adopts camera as information acquisition unit. It has the advantages of non-intrusiveness and less interference to the drivers. Therefore, at present, it is one of the most widely

used methods among ADAS applications. Meanwhile, researches show that there are strong correlations between PERCLOS features and driver fatigue, which is recognized as one of the most effective way to detect driver fatigue [8].

At present, driver fatigue identification algorithm mainly includes Bayesian network [9], neural network [10, 11], and HMM [12, 13]. Among them, HMM is regarded as an effective method due to its advantages of dynamic description capacity. However, in the model training process, the initial value selection of confusion matrix has a great influence on the model accuracy, and the model parameters easily fall into local optimum due to the initial value determined in advance. Therefore, it is important to solve this problem for the driver's fatigue detection.

Based on above analyses, this study focused on how to improve HMM training robustness by proposal of a dynamic fatigue detection model, in which the particle swarm optimization (PSO) algorithm was introduced into HMM training process to solve the problems of sensitive dependence on confusion matrix initial value. In addition, this study, paid more attention to the model robustness than that of its accuracy; thereby, only two hidden states of fatigue and alert were verified and analyzed in detail.

The rest of this paper is organized as follows: section II introduces the method of driver fatigue identification, including features and HMM analysis; section III describes the HMM designed for driver fatigue; experiments and analysis are carried out in section IV; and final conclusions are derived with suggestions for further study.

## II. METHODS

Generally, the HMM construction can be divided into three steps: feature factors analysis, HMM structure design and relevant parameters optimization.

### 2.1. Feature Analysis

As descriptions in section I, driver fatigue can be inferred from facial expression or observable variables extracted when fatigue occurs. As there are so many factors that affect fatigue, it is impossible to include all of them into the proposed models. Meanwhile, in consideration of the main purpose of this paper which aims to improve the robustness of the HMM with PSO algorithm, here only the most significant feature, PERCLOS, which is defined as the percentage of eye closing time over a certain period [14] is incorporated. In general, PERCLOS feature is consist of three variables: P70, P80 and EM. These variables describe the proportion of time that the eyes are closed at least 70%, 80% and 50% respectively. In which, P80 has been proved its correlation with fatigue level. Therefore, it is widely used as standard for some fatigue identification system. Fig. 1 provides an illustration to explain

\*This project is supported by National Natural Science Foundation of China (Grant No. 51675077), China Postdoctoral Science Foundation (No. 2017T100178, 2015M581329), and the Fundamental Research Funds for the Central Universities (No. DUT16QY42).

M. Zhang is with the State Key Laboratory of Structural Analysis for Industrial Equipment, and the School of Automotive Engineering, Dalian University of Technology, Dalian 116022, China (phone: 15542361218; e-mail: gloriashang@163.com).

X. Zhai, G. Zhao, and T. Chong are with the School of Automotive Engineering, Dalian University of Technology, Dalian 116022, China (e-mail: 1354452490@qq.com).

Z. Wang is with the Institute of Industrial Science, The University of Tokyo, Tokyo, 153-8505, Japan (e-mail: z-wang@iis.u-tokyo.ac.jp).

this variable. Where  $t_1$  is the time from when the eyes are fully opened to when they are closed 20%, and this time period is defined as the state of the eyes opened according to the P80 standard.  $t_2$  is the time from when the eyes are fully opened to when they are closed 80%.  $t_3$  is the time from when the eyes are fully opened to when they are opened 20% again.  $t_4$  is the time from when the eyes are fully opened to when they are opened 80% again. And the definition of P80 is as follow:

$$P80 = \frac{t_3 - t_2}{t_4 - t_1}, \quad (1)$$

where  $t_3 - t_2$  represents the total time when the eyes were closed more than 80%, and  $t_4 - t_1$  represents the total time of the blinking process.

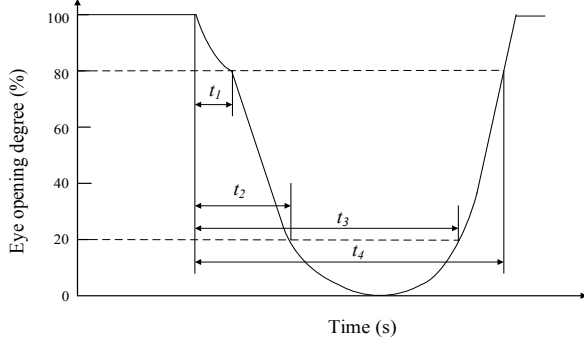


Figure 1. Sketch of PERCLOS.

## 2.2. HMM Analysis

In general, the generic HMM can be described as  $\lambda = (\pi, A, B)$ . In which, it consists of two random processes: one is the Markov process, which is described with initial probability  $\pi$  and transition probability matrix  $A$ . It directly reflects the changes of hidden state sequences. The other is the random process of observations, which is described with confusion matrix  $B$ . For discrete solutions, the initial parameters  $\pi$  and matrix  $A$  have less effect on the model accuracy. So they can be determined with random or uniform distributions under the following conditions:

$$\begin{cases} 0 \leq a_{i,j} \leq 1, \sum_{j=1}^n a_{i,j} = 1, \\ \pi_i = P(q_i = \theta_i), 1 \leq i \leq n \end{cases} \quad (2)$$

where  $a_{i,j}$  denotes the state transition probability from  $i$  to  $j$ , and  $P(q_i = \theta_i)$  denotes the probability that state  $q$  belongs to  $\theta$  in Markov chain at time  $t$ .

For matrix  $B$ , its initial value has significant influence on the model accuracy. Researchers showed that the main reason lies in the Baum-Welch (BW) algorithm [15] which is often used for the HMM training process. This method is easy to fall into the local optimum solutions. Thus, it is necessary to select an appropriate initial value for matrix  $B$  to make the model training process robust, which is inconvenient in practical applications.

Considering that PSO is easy to realize, and it has the advantages of finding global optimum solutions, high

accuracy and fast convergence, we introduced PSO algorithm to optimize the model training process.

## 2.3. PSO Algorithm

The basic idea of PSO algorithm is to find the optimal target value through cooperation and information sharing among individuals in a group. The number of particles depends on the complexity of the problem. The more complex the problem, the more particles are selected. For continuous optimal problem, the speed and position of the particle are updated by comparing two conditions (global optimal solution  $gbest$  and individual optimal solution  $pbest$ ).

$$\begin{cases} V_i = w \times V_i + c_1 \times rand \times (pbest_i - X_i) + c_2 \times rand \times (gbest_i - X_i), \\ X_i = X_i + V_i \end{cases} \quad (3)$$

where  $w$  is a non-negative number and it is related to the global optimization ability,  $V_i$  represents the velocity of particles,  $rand$  is a random number between (0,1),  $X_i$  is the current position of particles, and  $c_1$  and  $c_2$  are the learning factors both usually set as 2.

## 2.4. Consistency Analysis of HMM

Consistency analysis is important for the model's accuracy. In this paper, the most probable state sequence  $\hat{Q}$  can be obtained with the improved method. Then, it is tested through comparing with the real sequence  $Q$  which is acquired through fusing the information of heart rate test and subjective evaluation. The analysis process consists of two aspects:

(1) Calculate the similarity between  $\hat{Q}$  and  $Q$ . For instance, assume the length of the sequence is  $n$ , and the superimposed number is  $s$ , then the similarity  $S_i$  is:

$$S_i = \frac{s}{n} \times 100\% \quad (4)$$

(2) Calculate the variance  $Var$  of vector  $X$ . Assume  $X = \hat{Q} - Q$ , and  $V = \sum_{i=1}^n X_i / n$ , then the variance of  $X$  is:

$$Var = \frac{1}{n} \sum_{i=1}^n (X_i - V)^2 \quad (5)$$

## III. DRIVER FATIGUE MODEL

In this paper, the fatigue HMM construction can be divided into three steps: hidden state definition, HMM structure design and model construction.

### 3.1. Hidden State Definition

In consideration of the main purpose of this paper, we define the hidden state as fatigue and alert. So the observable variables can be divided into two states: normal and abnormal. According to previous researches [16], here the threshold of PERCLOS is set as 0.15. Table I shows the definition of the observable variables and the hidden state.

TABLE I. PARAMETERS DEFINITION

Variables	abnormal	normal	State	fatigue	alert
-----------	----------	--------	-------	---------	-------

PERCLOS	1	2	Level	1	2
---------	---	---	-------	---	---

### 3.2. HMM Structure Design

Based on the analysis in section 2.2, we assume matrix  $A$  as uniform or random distribution. For convenience sake, the initial values of matrix  $B$  are divided into two cases according to whether there is a prior condition or not. The prior condition can be described as: assume  $M$  as the sequence length of observable states, and  $Q$  as the length of real states. Based on the proper statistics, we can obtain the number  $Q_j$  of the real state  $j$  within this period of time and the number  $M_{jk}$  of the observable state  $k$ . Then, the elements of matrix  $B$  is:

$$b_{jk} = \frac{M_{jk}}{Q_j}, \sum_{k=1}^2 M_{jk} = Q_j, j = 1, 2. \quad (6)$$

Based on above analysis, the parameters of three HMM used in this paper are listed as Table II.

TABLE II. PARAMETERS INITIALIZATION FOR DIFFERENT MODELS

Parameters Models	Transition matrix $A$	Confusion matrix $B$
1-BW	<i>uniform distribution</i>	<i>random distribution</i>
	$A_0 = \begin{pmatrix} 0.5 & 0.5 \\ 0.5 & 0.5 \end{pmatrix}$	$B_0 = \begin{pmatrix} 0.3 & 0.7 \\ 0.6 & 0.4 \end{pmatrix}$
2-BW	<i>uniform distribution</i>	<i>prior distribution</i>
	$A_0 = \begin{pmatrix} 0.5 & 0.5 \\ 0.5 & 0.5 \end{pmatrix}$	$B_0 = \begin{pmatrix} 0.73 & 0.27 \\ 0.07 & 0.93 \end{pmatrix}$
3-BW-PSO	<i>random distribution</i>	<i>random distribution</i>
	$A_0 = \begin{pmatrix} r_{a11} & 1 - r_{a11} \\ r_{a21} & 1 - r_{a21} \end{pmatrix}$	$B_0 = \begin{pmatrix} r_{b11} & 1 - r_{b11} \\ r_{b21} & 1 - r_{b21} \end{pmatrix}$

### 3.3. Construction of HMM

For the model 1 and 2, based on the parameters initialization, the optimal matrices  $A$  and  $B$  can be obtained by iterative procedure with the following equation:

$$\begin{cases} \hat{a}_{ij} = \frac{\sum_{t=1}^{T-1} \varepsilon_t(i, j)}{\sum_{t=1}^{T-1} \gamma_t(i)} \\ \hat{b}_j(k) = \frac{\sum_{t=1, o_t=k}^T \gamma_t(j)}{\sum_{t=1}^T \gamma_t(j)} \end{cases}, \quad (7)$$

where  $\sum_{t=1}^{T-1} \varepsilon_t(i, j)$  represents the expected number of times from state  $s_i$  to  $s_j$ ,  $\sum_{t=1}^{T-1} \gamma_t(i)$  represents the expected number of times transferred from state  $s_i$ , and  $k$  represents the classified state of observable variables.

For the model 3, we introduced PSO algorithm into the HMM training process. The basic process is shown in Fig. 2.

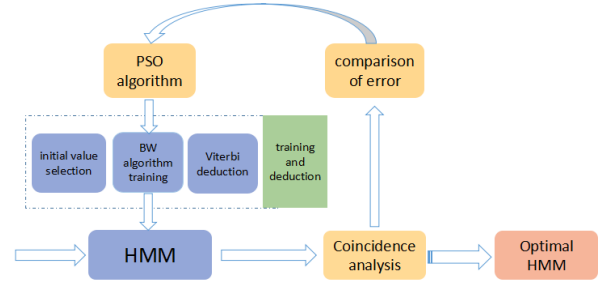


Figure 2. Sketch of BW-PSO for HMM training.

The main steps of BW-PSO are described as follows:

(1) Initialization: according to training scale, randomly generate  $n$  initial matrix including transition probability matrix  $A_0$  and confusion matrix  $B_0$ .

(2) Initial value selection: the updated transition probability matrix  $A_1$  and confusion matrix  $B_1$  can be obtained through BW algorithm.

(3) Fitness function: based on all updated  $A_1$  and  $B_1$ , the maximum estimation state series  $\hat{Q} = \{\hat{q}_1, \hat{q}_2, \dots, \hat{q}_i\}$ ,  $i = 1, 2, \dots, n$  can be acquired through maximum possible state estimation steps. Assume  $Q = \{q_1, q_2, \dots, q_i\}$  as the real state series, we define the variance  $\delta$  of  $X = \hat{Q} - Q$  as the fitness function:

$$\delta = \frac{\sum_{i=1}^n (X_i - \bar{X})^2}{n}. \quad (8)$$

(4) Particle's position and velocity update: the particle's position and velocity can be adjusted based on the new fitness value  $\delta$ , and the new position and velocity can be determined with the following description:

$$\begin{cases} x_{i,t+1}^d = x_{i,t}^d + v_{i,t+1}^d \\ v_{i,t+1}^d = \omega v_{i,t}^d + c_1 \cdot rand \cdot (p_{i,t}^d - x_{i,t}^d) + c_2 \cdot rand \cdot (p_{g,t}^d - x_{i,t}^d) \end{cases}, \quad (9)$$

where  $\vec{X}_i = (x_{i1}, x_{i2}, \dots, x_{id}, \dots, x_{iD})$  denotes each particle's coordinate position vector in  $D$  dimensional space,  $\vec{V}_i = (v_{i1}, v_{i2}, \dots, v_{id}, \dots, v_{iD})$  denotes each particle's velocity vector, and  $\vec{P}_i = (p_{i1}, p_{i2}, \dots, p_{id}, \dots, p_{iD})$  is the optimum position of each particle. Then the best position of the swarm is  $\vec{P}_g = (p_{g1}, p_{g2}, \dots, p_{gd}, \dots, p_{gD})$ .

(5) Termination condition: In this paper, the termination condition is that the evolution generation reaches the maximum training times  $T_{max}$ .

The parameters of PSO algorithm are listed in the Table III.

TABLE III. PARAMETERS OF PSO ALGORITHM

Parameter	$n$	$w$	$c_1$	$c_2$	$T_{max}$
Value	10	0.9	2	2	90

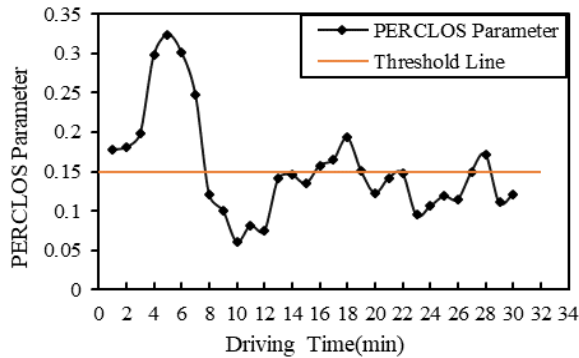
## IV. EXPERIMENT AND RESULTS

### 4.1. Driving Experiment

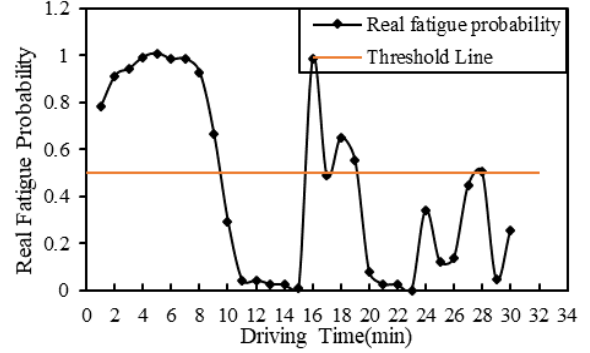
In this study, 20 volunteers aged 24 - 26 who have 2 - 3 years' driving experience participated in the experiments. During the experiment, each participant was asked to operate the driving simulator from 1:00 P.M to 3:00 P.M, at speed of 90km/h in highway environment. The highway scenario in driving simulator is shown in Fig. 3. The PERCLOS data sequence was sampled at one minute through Head-Mounted Eye Tracker SMI-HED. To reduce the calculation complexity, we divide the parameter data into 30-minute units, each of which represents a set of observations. Therefore, for one person, we can get 4 sets of observations, for 20 participants, a total of 80 observations. Of these, 60 are for model training and 20 are for model testing. Fig. 4a shows the PERCLOS data distribution of a random sample along with the change of driving time. Based on the analysis in section 3.1, we know that a PERCLOS value greater than 0.15 indicates that the driver is in the fatigue state. So, it can be seen that, within the selected period, the driver's state changes with the following sequence: 'fatigue-alert-fatigue-alert'. Fig. 4b is the real fatigue probability curve over the same time period which is acquired through fusing the information of heart rate test and subjective evaluation, and the driver's real state changes with the following sequence: 'fatigue-alert-fatigue-alert'. Comparing the two figures, we can see that the trend of PERCLOS is basically in line with the trend of the real state of the driver. So, PERCLOS is suitable for testing the robustness of the proposed models.



Figure 3. Highway scenario in the driving simulator experiment.



(a) PERCLOS curve



(b) Real fatigue probability curve

Figure 4. PERCLOS and real fatigue probability of a random sample for driver fatigue detection: (a) PERCLOS curve, and (b) real fatigue probability curve.

### 4.2. Analysis of Model Training Results

Based on the above experiment data and analysis, the parameters optimization curves are shown in Fig. 5. In which, considering the sum of each row's elements in matrix  $A$  and  $B$  is equal to 1, so only the first column's elements are chosen for comparison. Table IV and Table V listed the whole time consumption for the parameters optimization process and the final optimized solutions respectively.

Based on the results comparison for the above three models, some conclusions can be drawn:

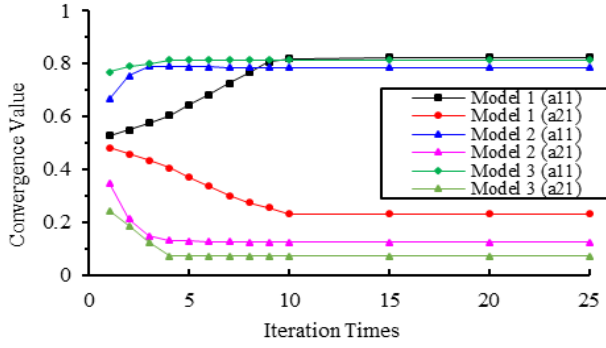
(1) For matrix  $A$ , the iterative process is uniformly convergent. The initial value of matrix  $A$  has little influence on the accuracy of the proposed models. But, to some extent, the element initialization method based on prior condition (corresponding to model 2) and PSO (corresponding to model 3) can accelerate the training process.

(2) For matrix  $B$ , the iterative process differs quite a bit in the model training result, even the wrong solutions are given out (shown as the model 1 in Fig. 5b, the elements  $b_{11}$  and  $b_{21}$  of model 1 differ greatly from the elements of the other two models.) When the elements of matrix  $B$  are initialized as random distribution, the iterative process is easy to fall into a local optimal solution and leads to a large error within the training process. However, for model 3, the element initial method has little influence on the accuracy and the PSO method can accelerate the training process.

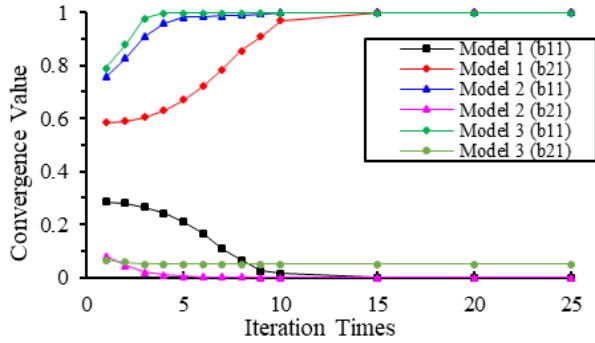
(3) For the method of prior condition (corresponding to model 2) and PSO (corresponding to model 3), they both can effectively reduce the number of iterations, but the time consumption of PSO method is much larger than the others. That means the method based on BW-PSO can be accepted for small-scale problems. When the computing complexity increasing with problem size, we must make a compromise between computation scales and accuracy.

(4) For model 1 (BW method), the accuracy of the parameter optimization process is largely dependent on matrix  $B$  initialization. On the other hand, for model 2 and 3, the accuracy is more robust. However, for model 2, as there is some prior condition need to be determined in advanced, it is necessary to analysis the strategy for different problems. By

contrast, model 3 has great advantages in accuracy and robustness. So it is more suitable for automation processing.



(a) Parameter optimization for matrix  $A$



(b) Parameter optimization for matrix  $B$

Figure 5. Parameter optimization for matrix  $A$  and  $B$ : (a) parameter optimization for matrix  $A$ , and (b) parameter optimization for matrix  $B$ .

TABLE IV. THE STATISTICS OF TIME CONSUMPTION

Models	1-BW	2-BW	3-BW-PSO
Time (ms)	99.61	14.99	601.66

TABLE V. OPTIMIZED SOLUTIONS FOR THE PROPOSED MODELS

Parameters Models	Transition matrix $A$	Confusion matrix $B$
1-BW	$A_{BW1}$ $= \begin{pmatrix} 0.8235 & 0.1765 \\ 0.2308 & 0.7692 \end{pmatrix}$	$B_{BW1}$ $= \begin{pmatrix} 0.0000 & 1.0000 \\ 1.0000 & 0.0000 \end{pmatrix}$
2-BW	$A_{BW2}$ $= \begin{pmatrix} 0.7857 & 0.2143 \\ 0.1250 & 0.8750 \end{pmatrix}$	$B_{BW2}$ $= \begin{pmatrix} 1.0000 & 0.0000 \\ 0.0000 & 1.0000 \end{pmatrix}$
3-BW-PSO	$A_{BW-PSO}$ $= \begin{pmatrix} 0.8128 & 0.1872 \\ 0.0708 & 0.9292 \end{pmatrix}$	$B_{BW-PSO}$ $= \begin{pmatrix} 0.9977 & 0.0023 \\ 0.0488 & 0.9512 \end{pmatrix}$

#### 4.3. Analysis of Model Identification Results

In order to verify the accuracy and robustness of the proposed methods, in this section, we will make a detailed analysis for each model based on two cases.

(1) Randomly select 1 set of observations for identification and verify the accuracy. Considering the

dependence of the three models on the matrix initialization, so we compared the statistical result of the model's output in accuracy under the following conditions. For model 1 and 3, matrix  $A$  and  $B$  were initialized as random distribution. For model 2, considering it is a particular case of model 1 (in fact, model 2 is a specific case of model 1 under certain conditions), so we firstly extracted the prior condition for matrix  $B$  and then imported this information into the matrix initialization steps. The detailed analysis results are shown in Table VI.

TABLE VI. STATISTICAL RESULT OF THE MODEL ACCURACY

Reference	1111122222 2221111122 22221112 <sup>a</sup>	Non-matches	Accuracy (%)	Var
1-BW	$\begin{bmatrix} 222222 & 2111 \\ 1111 & 2222 \\ 111111 & 1211 \end{bmatrix}$	25	16.7	0.85
2-BW	$\begin{bmatrix} 111111 & 2222 \\ 2222 & 1111 \\ 2222 & 2221 \end{bmatrix}$	7	76.7	0.23
3-BW-PSO	$\begin{bmatrix} 111111 & 2222 \\ 2222 & 1111 \\ 2222 & 2222 \end{bmatrix}$	6	80.0	0.19

a. "1" indicates fatigue and "2" indicates alert.

From the above statistical result, some conclusions can be made: Firstly, due to the accuracy and robustness of model 1 is largely dependent on the matrix initialization, certain prior conditions must be used to improve the identification accuracy in the practical application. Secondly, in the test result, accuracy and variance of model 3 are the best. However, it is important to note that Model 3 consumes significantly more time than Model 2 during model training. This can be seen from the time consumption result in Table IV.

(2) In order to further test the robustness of the proposed methods, based on the above analysis result described in case 1, we randomly selected 10 sets of observations from the test set and then analyzed them respectively. The result of the comparison between the proposed models are shown in Fig. 6. It can be observed that, for the given test data, the accuracy of the prediction results for model 1 varies widely and the robustness is poor, and even in some cases, accurate output cannot be obtained. However, for Model 2 and Model 3, the overall accuracy shows little change and the robustness is better, and the accuracy of both models can reach more than 0.7. Furthermore, model 3 is better than model 2 in terms of accuracy and stability.

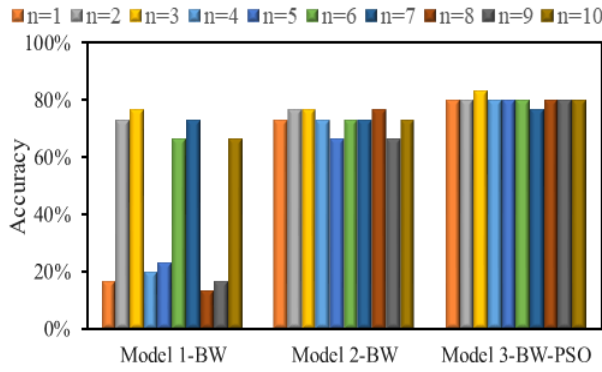


Figure 6. Contrast Diagram of the change of three models' accuracy (n represents the serial number of the selected test sequence).

## V. CONCLUSION

In practical applications with HMM, the initial conditions of HMM have a great influence on the training process and accuracy. Based on this consideration, this paper aims to improve the HMM training process by application of a particle swarm optimization method. Particularly, based on the generation process of driver fatigue, a HMM framework was constructed for driver fatigue identification, which was tested with experimental data. The testing results show that the proposed BW-PSO method can achieve the global optimum solutions without specific matrix initialization process, which can bring a great convenience to the practical applications.

In the future work, the proposed driver fatigue identification model will be extended with multiple information fusion, to make the model more conducive for practical applications.

## REFERENCES

- [1] A. Smith and H. Smith, "Perceptions of risk factors for road traffic accidents," *Advances in Social Sciences Research Journal*, vol. 4, no. 1, pp. 140-146, 2017.
- [2] H. Wang, C. Zhang, T. Shi, F. Wang, and S. Ma, "Real-time EEG-based detection of fatigue driving danger for accident prediction," *International Journal of Neural Systems*, vol. 25, no. 02, 1550002, 2015.
- [3] T.L.T. da Silveira, A.J. Kozakevicius, and C.R. Rodrigues, "Automated drowsiness detection through wavelet packet analysis of a single EEG channel," *Expert Systems with Applications*, vol. 55, pp. 559-565, 2016.
- [4] P. P. San, S. H. Ling, R. Chai, Y. Tran, A. Craig, and H. Nguyen, "EEG-based driver fatigue detection using hybrid deep generic model," in *38th Annual International Conference of the IEEE Engineering in Medicine and Biology Society*, 2016, pp. 800-803.
- [5] R. Fu, H. Wang, Y. Zhang, and F. Wang, "An analysis on EMG and ECG signals for driving fatigue detection based on wearable sensor," *Automotive Engineering*, vol. 35, no. 12, pp. 1143-1148, 2013. (in Chinese)
- [6] W. Li, Q. He, and X. Fan, "Detection of driver's fatigue based on vehicle performance output," *Journal of Shanghai Jiaotong University*, vol. 44, no. 2, pp. 292-296, 2010. (in Chinese)
- [7] W. Zhang, Z. Wang, and Y. Li, "Illumination compensation of color image for driver facial features detection," *International Journal of Digital Content Technology and its Applications*, vol. 6, no. 17, pp. 475-482, 2012.
- [8] D. F. Dinges and P. R. Grace, "A valid psychophysiological measure of alertness as assessed by psychomotor vigilance," Report No. FH-WA2MCRT2982006, Federal Highway Administration, Office of Motor Carriers, 1998.

- [9] W. Guo, B. Zhang, L. Xia, S. Shi, X. Zhang, and J. She, "Driver drowsiness detection model identification with Bayesian network structure learning method," in *2016 IEEE Control and Decision Conference*, 2016, pp. 131-136.
- [10] K. R. Sinha, "Artificial neural network and wavelet based automated detection of sleep spindles, REM sleep and wake states," *Journal of Medical Systems*, vol. 32, no. 4, pp. 291-299, 2008.
- [11] C. Yan, H. Jiang, B. Zhang, and F. Coenen, "Recognizing driver inattention by convolutional neural networks," in *8th IEEE International Congress on Image and Signal Processing*, 2015, pp. 680-685.
- [12] R. Fu, H. Wang, and W. Zhao, "Dynamic driver fatigue detection using hidden Markov model in real driving condition," *Expert Systems with Applications*, vol. 63, pp. 397-411, 2016.
- [13] Y. Xiang, "Eye Fatigue State Recognition of Gabor Wavelet Optimization HMM Algorithm," *International Journal of Hybrid Information Technology*, vol. 9, no. 9, pp. 189-198, 2016.
- [14] L. E. Baum, T. Petrie, G. Soules, and N. Weiss, "A maximization technique occurring in the statistical analysis of probabilistic functions of Markov chains," *The Annals of Mathematical Statistics*, vol. 41, no. 1, pp. 164-171, 1970.
- [15] M. Elmezain, A. Al-Hamadi, J. Appenrodt, and B. Michaelis, "A hidden Markov model-based continuous gesture recognition system for hand motion trajectory," in *19th IEEE International Conference on Pattern Recognition*, 2008, pp. 1-4.
- [16] J. Xie, M. Xie, and W. Zhu, "Driver fatigue detection based on head gesture and PERCLOS," in *2012 IEEE International Conference on Wavelet Active Media Technology and Information Processing*, 2012, pp. 128-131.